PERGAMON

Computers and Structures 79 (2001) 1977–1985

Computers & Structures

www.elsevier.com/locate/compstruc

Topology optimization of structures with geometrical nonlinearities

Hae Chang Gea *, Jianhui Luo

Department of Mechanical and Aerospace Engineering, The State University of New Jersey, 98 Brett Road, Piscataway, NJ 08855, USA

Received 27 November 2000; accepted 22 June 2001

Abstract

In this paper, the stiffness optimization problem is investigated for structures with geometrical nonlinearities. The mean compliance of the structure is chosen as the objective function and its sensitivities are derived using the adjoint method. The optimal problem is formulated using a microstructure-based design domain method and is solved iteratively by a sequential convex approximation method. Three numerical examples are presented to show the applications of the proposed method and the results demonstrate that the geometrically nonlinear finite element analysis is indispensable to the optimization process of large displacement structures. © 2001 Published by Elsevier Science Ltd.

Keywords: Topology optimization; Geometrical nonlinearity; Sensitivity analysis

1. Introduction

Structural optimization is rapidly becoming an integral part of the product design process. Given today's timing and budget constraints, structural optimization yields a significantly superior design than the conventional trial and error approach. Two types of structural optimization problems at the level of macroscopic design can be categorized from the literature: sizing/shape optimization and topology optimization [5]. Sizing/shape optimization provides the means to generate optimal designs by modifying geometrical parameters without violating the integrity of the structure topology, therefore the topology of the structure is predefined and remains unchanged throughout. Topology optimization, however, does not require an initial design as input. Given a specified region, loads, and boundary conditions, the most structurally efficient material layout is determined. Considerable efforts has also been extended to the inverse material design problems.

While the traditional structural optimization mainly deals with geometry optimization problems, topology optimization has drawn more and more attentions recently. In the context of topology modeling technique, Bendsøe and Kikuchi [3] introduced a micro-structure based homogenization method, Bendsøe [4] and Rozvany and Zhou [19] proposed a density function approach, and Gea [11] derived a design domain method which retains the merits from both the homogenization method and the density function approach. As far as topology optimization applications are concerned, Suzuki and Kikuchi [22] considered shell structures and 3D linear elastic problems for stiffness optimization; Diaz and Kikuchi [9], Ma et al. [16] studied vibration problems under various objective functions. Nonsmoothness of eigenvalue problems have been studied by Seyranian et al. [20]; stability problems were studied by Neves et al. [18], and the design of compliant mechanisms using topology optimization has also been investigated intensively [1,21]; Luo and Gea [12–15] and Yang et al. [24] studied the optimal stiffener design of shell/plate structures; the topology optimization was also used for the noise reduction [13]. A complete literature review can be found in Ref. [5].

Despite its wide applications in mechanical design, the majority of the topology optimization problems use the linear finite element analysis to find the structure responses, which inherently assumes that the structures

* Corresponding author. Tel./fax: +1-732-445-0108.
E-mail address: gea@rci.rutgers.edu (H.C. Gea).

0045-7949/01/$ - see front matter © 2001 Published by Elsevier Science Ltd.
PII: S0045-7949(01)00117-1

can only undergo small displacements. This assumption is applicable to a large class of problems, however, it is not always valid, such as in the case of compliant mechanism design and crashworthiness design. For structural design involving large displacements or/and large rotations, it is necessary to consider the geometrically nonlinear finite element analysis. Compared to vast publications on small displacement topology optimization, very limited research works have been done on large displacement optimization [6,7].

In this work, the stiffness optimization problem is considered for geometrically nonlinear structures under full loads. The mean compliance is chosen as the objective function and its sensitivities are derived using the adjoint method. The microstructure-based design domain method [11] is employed to formulate the optimization problem which is then solved iteratively by a sequential convex approximation method called generalized convex approximation (GCA) [8]. Three numerical examples are presented to showcase the significant differences between the designs obtained from large displacement analysis and from small displacement analysis.

The remainder of the paper is organized as follows: Section 2 proposes the basic problem of the geometrically nonlinear analysis and discusses its solution techniques. In Section 3, the relations between the mean compliance, the strain energy and the complementary strain energy of large displacement structures are derived, which follows the discussion of the microstructure-based design domain method. By using the adjoint method, the derivations of the mean compliance with respect to the design variables are also formulated. Section 4 presents the numerical results of the proposed approach in comparison with those from small displacement analysis. Some concluding remarks are made in Section 5.

2. Geometrically nonlinear analysis

2.1. The basic problem

Consider large displacement motion of a general body subjected to applied body forces f^{B}, surface tractions f^{S} on the surface ${}^0S_f$, and the displacement boundary condition ${}^0S_u$. We assume the load is applied all together and both the force and displacement boundary condition are deformation independent. The Lagrangian approach is adopted to formulate the problem because the Lagrangian formulation usually represents a more natural and effective analysis approach than an Eulerian formulation in the analysis of solids and structures. In Lagrangian approach, the equilibrium of the body can be expressed using the principle of virtual displacements as [2]

$$\int_{{}^0V} S_{ij}\delta\epsilon_{ij}\,\mathrm{d}^0V = \int_{{}^0V} f_i^{\mathrm{B}}\delta u_i\,\mathrm{d}^0V + \int_{{}^0S_f} f_i^{\mathrm{S}}\delta u_i^{\mathrm{S}}\,\mathrm{d}^0S \tag{1}$$

where S_{ij} are Cartesian components of the second Piola–Kirchhoff stress tensor, $\delta\epsilon_{ij}$ are components of Green–Lagrange strain tensor corresponding to virtual displacements δu_i, δu_i^{S} are virtual displacements evaluated on the surface ${}^0S_f$. ${}^0V$ denotes the body volume at initial configuration. The Green–Lagrange strain tensor is defined with respect to the initial coordinates of the body, and in the form of

$$\epsilon_{ij} = \frac{1}{2}\left(\frac{\partial u_i}{\partial {}^0x_j} + \frac{\partial u_j}{\partial {}^0x_i} + \frac{\partial u_k}{\partial {}^0x_i}\frac{\partial u_k}{\partial {}^0x_j}\right) \tag{2}$$

If strains are reasonably small we can still write the general elastic constitutive relation

$$S_{ij} = C_{ijkl}\epsilon_{kl} \tag{3}$$

where C_{ijkl} are the components of the constant elasticity tensor.

Eqs. (1)–(3) are the basic equations for calculating the structural responses in geometrically nonlinear analysis, however they cannot be solved directly due to high degree of nonlinearities. One remedy to this difficulty is to linearize the equilibrium equation of Eq. (1) to find an approximate solution and then gradually reduce the approximation by iteration. While it is possible to accomplish the solutions for a full load in a one-step operation, an incremental analysis is often used to avoid nonunique and physically unimportant solutions. In the incremental analysis, the load is gradually incremented and the nonlinear structural responses for each increment are sought. Despite the cost associated with the calculations at the intermediate steps, the incremental approach is usually computational cheaper as effects of nonlinearity in each step are reduced.

2.2. Linearized incremental equation

In the incremental analysis, we seek the structural responses at state $t+\Delta t$ based on the known results at state t. Here, t is not a time variable, it is only a convenient variable which denotes different intensities of load applications and correspondingly different configurations. By introducing the increments, the displacements, strains and stresses at state $t+\Delta t$ can be decomposed as

$${}^{t+\Delta t}u_i = {}^tu_i + \Delta u_i \tag{4}$$

$${}^{t+\Delta t}\epsilon_{ij} = {}^t\epsilon_{ij} + \Delta\epsilon_{ij} \tag{5}$$

$${}^{t+\Delta t}S_{ij} = {}^tS_{ij} + \Delta S_{ij} \tag{6}$$

where ${}^{t}u_i$, ${}^{t}\epsilon_{ij}$ and ${}^{t}S_{ij}$ are the displacements, strains and stresses at state t, which are pre-calculated, Δu_i, $\Delta\epsilon_{ij}$ and ΔS_{ij} are the corresponding increments to be determined.

It should be noted that Eqs. (1)–(3) are satisfied during the entire loading course. Insert Eq. (4) into the strain–displacement relation Eq. (2) and make use of Eq. (5), we have

$$\Delta\epsilon_{ij} = e_{ij} + \eta_{ij} \tag{7}$$

where e_{ij} represents the linear incremental strain

$$e_{ij} = \frac{1}{2}\left(\frac{\partial\Delta u_i}{\partial^0 x_j} + \frac{\partial\Delta u_j}{\partial^0 x_i} + \frac{\partial^t u_k}{\partial^0 x_i}\frac{\partial\Delta u_k}{\partial^0 x_j} + \frac{\partial\Delta u_k}{\partial^0 x_i}\frac{\partial^t u_k}{\partial^0 x_j}\right) \tag{8}$$

and η_{ij} stands for the nonlinear incremental strain

$$\eta_{ij} = \frac{1}{2}\frac{\partial\Delta u_k}{\partial^0 x_i}\frac{\partial\Delta u_k}{\partial^0 x_j} \tag{9}$$

Noting that $\delta^{t+\Delta t}u_i = \delta\Delta u_i$, $\delta^{t+\Delta t}\epsilon_{ij} = \delta\Delta\epsilon_{ij}$ as the variation is taken about the configuration at state $t+\Delta t$, and also noticing the decomposition in Eq. (6), equilibrium equation pertaining to state $t+\Delta t$ can be written as

$$\begin{aligned}&\int_{{}^0V} \Delta S_{ij}\delta\Delta\epsilon_{ij}\,\mathrm{d}^0V + \int_{{}^0V} {}^{t}S_{ij}\delta\eta_{ij}\,\mathrm{d}^0V \\ &\quad= \int_{{}^0V} {}^{t+\Delta t}f_i^{\mathrm{B}}\delta\Delta u_i\,\mathrm{d}^0V + \int_{{}^0S_f} {}^{t+\Delta t}f_i^{\mathrm{S}}\delta\Delta u_i^{\mathrm{S}}\,\mathrm{d}^0S \\ &\qquad- \int_{{}^0V} {}^{t}S_{ij}\delta e_{ij}\,\mathrm{d}^0V\end{aligned} \tag{10}$$

Using the approximations $\Delta S_{ij} = C_{ijkl}e_{kl}$, $\delta\Delta\epsilon_{ij} = \delta e_{ij}$, we obtain the linearized incremental equation of motion

$$\begin{aligned}&\int_{{}^0V} c_{ijkl}e_{ij}\delta e_{kl}\,\mathrm{d}^0V + \int_{{}^0V} {}^{t}S_{ij}\delta\eta_{ij}\,\mathrm{d}^0V \\ &\quad= \int_{{}^0V} {}^{t+\Delta t}f_i^{\mathrm{B}}\delta\Delta u_i\,\mathrm{d}^0V + \int_{{}^0S_f} {}^{t+\Delta t}f_i^{\mathrm{S}}\delta\Delta u_i^{\mathrm{S}}\,\mathrm{d}^0S \\ &\qquad- \int_{{}^0V} {}^{t}S_{ij}\delta e_{ij}\,\mathrm{d}^0V\end{aligned} \tag{11}$$

the right-hand side in Eq. (11) represents an "out-of-balance virtual work" of the system, which is due to the approximation we introduced while performing the linearization of the equilibrium equation; the left-hand side of Eq. (11) defines the so-called tangent structure, which is a "virtual" structure contingent on structural displacement and stress field. Eq. (11) should be solved iteratively until the unbalanced virtual work vanishes. Considering Eq. (11) is of continuous form, it is wise to transform it to finite element formulation.

2.3. Finite element formulation

Denote $\Delta\boldsymbol{u}$ as the nodal displacement incremental vector and $\boldsymbol{e}$ as the linear incremental strain vector, in compliance with the definition in Eq. (8), we have

$$\boldsymbol{e} = (\boldsymbol{B}_{L0} + \boldsymbol{B}_{L1})\Delta\boldsymbol{u} \tag{12}$$

where $\boldsymbol{B}_{L0}$ and $\boldsymbol{B}_{L1}$ are the linear strain–displacement transformation matrices. $\boldsymbol{B}_{L0}$ is the matrix used in linear infinitesimal strain analysis and $\boldsymbol{B}_{L1}$ depends on the displacement. The first and last terms of Eq. (11) can then be expressed in terms of the nodal incremental of displacements

$$\begin{aligned}\int_{{}^0V} c_{ijkl}e_{ij}\delta e_{kl}\,\mathrm{d}^0V = \Delta\boldsymbol{u}^{\mathrm{T}}\int_{{}^0V}(\boldsymbol{B}_{L0} + \boldsymbol{B}_{L1})^{\mathrm{T}}\boldsymbol{C}(\boldsymbol{B}_{L0} \\ + \boldsymbol{B}_{L1})\,\mathrm{d}^0V\delta\Delta\boldsymbol{u}\end{aligned} \tag{13}$$

$$\int_{{}^0V} {}^{t}S_{ij}\delta e_{ij}\,\mathrm{d}^0V = \int_{{}^0V} {}^{t}\overline{\boldsymbol{S}}(\boldsymbol{B}_{L0} + \boldsymbol{B}_{L1})\,\mathrm{d}^0V\delta\Delta\boldsymbol{u} \tag{14}$$

in which $\boldsymbol{C}$ is the elastic material matrix, and ${}^{t}\overline{\boldsymbol{S}}$ is the stress vector.

Define the nonlinear strain–displacement transformation matrix $\boldsymbol{B}_{NL}$ as

$$\nabla(\Delta\boldsymbol{u}) = \boldsymbol{B}_{NL}\Delta\boldsymbol{u} \tag{15}$$

here $\nabla(\Delta\boldsymbol{u})$ represents the displacement incremental gradient vector, for two-dimensional element

$$\nabla(\Delta\boldsymbol{u}) = \left(\frac{\partial\Delta u_1}{\partial^0 x_1}, \frac{\partial\Delta u_1}{\partial^0 x_2}, \frac{\partial\Delta u_2}{\partial^0 x_1}, \frac{\partial\Delta u_2}{\partial^0 x_2}\right)^{\mathrm{T}} \tag{16}$$

The second term in Eq. (11) can then be written as

$$\int_{{}^0V} {}^{t}S_{ij}\delta\eta_{ij}\,\mathrm{d}^0V = \Delta\boldsymbol{u}^{\mathrm{T}}\int_{{}^0V} \boldsymbol{B}_{NL}^{\mathrm{T}}\,{}^{t}\boldsymbol{S}\boldsymbol{B}_{NL}\,\mathrm{d}^0V\delta\Delta\boldsymbol{u} \tag{17}$$

where ${}^{t}\boldsymbol{S}$ denotes the second Piola–Kirchhoff stress matrix, in two-dimensional element formulation

$${}^{t}\boldsymbol{S} = \begin{bmatrix} {}^{t}S_{11} & {}^{t}S_{12} & 0 & 0 \\ {}^{t}S_{21} & {}^{t}S_{22} & 0 & 0 \\ 0 & 0 & {}^{t}S_{11} & {}^{t}S_{12} \\ 0 & 0 & {}^{t}S_{21} & {}^{t}S_{22} \end{bmatrix} \tag{18}$$

In the finite element analysis, all the external body forces and surface tractions need to be transformed to the nodal forces ${}^{t+\Delta t}\boldsymbol{R}$

$${}^{t+\Delta t}\boldsymbol{R}^{\mathrm{T}}\delta\Delta\boldsymbol{u} = \int_{{}^0V} {}^{t+\Delta t}f_i^{\mathrm{B}}\delta\Delta u_i\,\mathrm{d}^0V + \int_{{}^0S_f} {}^{t+\Delta t}f_i^{\mathrm{S}}\delta\Delta u_i^{\mathrm{S}}\,\mathrm{d}^0S \tag{19}$$

Substituting Eqs. (13), (14), (17) and (19) into the linearized incremental Eq. (11), we have

$${}^{t}\boldsymbol{K}_{\mathbf{T}}\Delta\boldsymbol{u} = (\boldsymbol{K}_0 + \boldsymbol{K}_{\mathbf{d}} + \boldsymbol{K}_{\boldsymbol{\sigma}})\Delta\boldsymbol{u} = \Delta\boldsymbol{F} \tag{20}$$

${}^{t}\boldsymbol{K}_{\mathbf{T}}$ is known as the tangent stiffness matrix, and $\Delta\boldsymbol{F}$ indicates the load unbalance between the external and internal forces

$$\Delta \boldsymbol{F} = {}^{t+\Delta t}\boldsymbol{R} - {}^{t}\boldsymbol{F} \tag{21}$$

with

$${}^{t}\boldsymbol{F} = \int_{{}_0V} (\boldsymbol{B}_{L0} + \boldsymbol{B}_{L1})^{\mathrm{T}}\, {}^{t}\overline{\boldsymbol{S}}\, \mathrm{d}^0V \tag{22}$$

$\boldsymbol{K}_0$ represents the usual, small displacement stiffness matrix, i.e.

$$\boldsymbol{K}_0 = \int_{{}_0V} \boldsymbol{B}_{L0}^{\mathrm{T}} \boldsymbol{C} \boldsymbol{B}_{L0}\, \mathrm{d}^0V \tag{23}$$

The matrix $\boldsymbol{K}_{\mathbf{d}}$ is due to the large displacement and is given by

$$\boldsymbol{K}_{\mathbf{d}} = \int_{{}_0V} (\boldsymbol{B}_{L0}^{\mathrm{T}} \boldsymbol{C} \boldsymbol{B}_{L1} + \boldsymbol{B}_{L1}^{\mathrm{T}} \boldsymbol{C} \boldsymbol{B}_{L0} + \boldsymbol{B}_{L1}^{\mathrm{T}} \boldsymbol{C} \boldsymbol{B}_{L1})\, \mathrm{d}^0V \tag{24}$$

$\boldsymbol{K}_{\mathbf{d}}$ is known as the large displacement matrix. $\boldsymbol{K}_{\boldsymbol{\sigma}}$ is a symmetric matrix dependent on the stress level and is known as the initial stress matrix, which is given by

$$\boldsymbol{K}_{\boldsymbol{\sigma}} = \int_{{}_0V} \boldsymbol{B}_{NL}^{\mathrm{T}}\, {}^{t}\boldsymbol{S} \boldsymbol{B}_{NL}\, \mathrm{d}^0V \tag{25}$$

The relation in Eq. (20) is employed to calculate an incremental in the displacements, which then is used to evaluate approximations to the displacements, strains and stresses corresponding to state $t + \Delta t$. The displacement approximations corresponding to $t + \Delta t$ are obtained simply by adding the calculated increments to the displacements at state t, and the strain and stress approximations are evaluated from the strain–displacement relation Eq. (2) and the constitutive relation Eq. (3) respectively. Once the approximate displacements, strains, and stresses have been obtained, we can check into how much difference there is between the external and internal forces from Eq. (21). In order to further reduce $\Delta \boldsymbol{F}$ we need to perform an iteration in which the above solution is repeated until $\Delta \boldsymbol{F}$ and $\Delta \boldsymbol{u}$ are negligible within a certain convergence measure. The calculated results at state $t + \Delta t$ are then used to find the structural response at the next loading level, and consequentially the final structural response under the full load can be obtained within certain steps.

3. Stiffness optimization

3.1. Optimization problem formulation

To design the stiffest structure under a given static loading, the mean compliance is adopted as the objective function. The stiffest structure is defined as a structure gives the least amount of displacement under loading and thus has the minimum mean compliance. The mean compliance W is defined as

$$W = \int_{{}_0V} f_i^{\mathrm{B}} u_i\, \mathrm{d}^0V + \int_{{}_0S_f} f_i^{\mathrm{S}} u_i^{\mathrm{S}}\, \mathrm{d}^0S \tag{26}$$

Obviously, W is also the work done by the external forces. For dead loads, we have the following work equation

$$W = U + U^{\mathrm{C}} \tag{27}$$

where U and U^{C} are the strain energy and its complementary energy. The strain energy U is defined as

$$U = \int_{{}_0V} \int S_{ij}\, \mathrm{d}\epsilon_{ij}\, \mathrm{d}^0V \tag{28}$$

and can be simplified by making use of the constitutive relation in Eq. (3)

$$U = \frac{1}{2} \int_{{}_0V} S_{ij} \epsilon_{ij}\, \mathrm{d}^0V \tag{29}$$

In order to derive the complementary strain energy U^{C}, we need to reformulate W in terms of stress and strain components. By choosing $\delta u_i = u_i$ in the equilibrium Eq. (1), and utilizing relations in Eqs. (2) and (26), we have

$$W = \int_{{}_0V} S_{ij} \left(\epsilon_{ij} + \frac{1}{2} \frac{\partial u_k}{\partial {}^0x_i} \frac{\partial u_k}{\partial {}^0x_j} \right) \mathrm{d}^0V \tag{30}$$

Subtracting Eq. (29) from Eq. (30), U^{C} can be formulated as

$$U^{\mathrm{C}} = U + \frac{1}{2} \int_{{}_0V} S_{ij} \frac{\partial u_k}{\partial {}^0x_i} \frac{\partial u_k}{\partial {}^0x_j}\, \mathrm{d}^0V \tag{31}$$

As we can see, the strain energy is not equal to its complementary energy in geometrically nonlinear structures even though the material is linear elastic. We recall in the infinitesimal displacement analysis, the strain energy is equal to its complementary energy, and the mean compliance is two-fold of the strain energy, therefore there is no bias to choose the mean compliance or the strain energy as the objective function in the stiffness optimization design. This is not the case in the geometrically nonlinear optimization, in which different choice of the objective functions will lead to different design results. In this study, we only consider the mean compliance as the objective function.

The optimization problem for stiffness optimization can then be formulated as

$$\begin{aligned} &\text{minimize} \quad W \\ &\text{subject to:} \quad \int_{{}_0V} \rho\, \mathrm{d}^0V \leqslant \Omega_s \end{aligned} \tag{32}$$

where ρ is the density distribution of the material and Ω_s stands for the upper bound of the given material.

3.2. Microstructure-based modeling

In the microstructure-based design domain method, the design domain is discretized into elements which are made of a composite material consisting of spherical micro-inclusions (voids) embedded in a solid matrix. The volume fractions of solid material in each of the design cells are considered as design variables.

The choice of spherical inclusions in an isotropic matrix ensures that the shape and orientation of the inclusion do not enter the problem formulation. The derivation of the density function is based on the work by Weng [23]. In his paper, the effective material properties are obtained using the Mori–Tanaka mean field theory [17] in conjunction with Eshelby's [10] equivalence principle and the solution for an ellipsoidal inclusion. For a composite material with a volume fraction z_i of the matrix material, the effective material properties of the composite are

$$\frac{\kappa_i}{\kappa_0} = 1 + \frac{(1-z_i)(\kappa_1-\kappa_0)}{z_i\alpha_0(\kappa_1-\kappa_0)+\kappa_0} \tag{33}$$

$$\frac{\mu_i}{\mu_0} = 1 + \frac{(1-z_i)(\mu_1-\mu_0)}{z_i\beta_0(\mu_1-\mu_0)+\mu_0} \tag{34}$$

where κ and μ are bulk and shear modulus, indices i represent the ith design element, 0 and 1 refer to the matrix and inclusion material respectively, and

$$\alpha_0 = \frac{1}{3}\frac{1+v_0}{1-v_0} \tag{35}$$

$$\beta_0 = \frac{2}{15}\frac{4-5v_0}{1-v_0} \tag{36}$$

here v_0 is the Poisson's ratio of the matrix. Since the inclusions are voids, κ_1 and μ_1 are set to be zero. Assuming $v_0 = 1/3$, the effective Young's modulus is

$$\frac{E_i}{E_0} = \frac{z_i}{2-z_i} = f(z_i) \tag{37}$$

The advantages of this method are that it is derived from the rigorous formulation of the theory of composite materials and gives a closed form expression for the effective Young's modulus, which is relatively simple to use.

3.3. Sensitivity analysis

In the gradient-based optimization approach, we need to determine the effects resulting from a small perturbation in the current design on the objective and constraint functions, which is known as the sensitivity analysis. Using the formulation in Eq. (26), the sensitivity of the mean compliance can be expressed as

$$\frac{\mathrm{d}W}{\mathrm{d}z_m} = \int_{{}^0V} f_i^{\mathrm{B}}\frac{\partial u_i}{\partial z_m}\,\mathrm{d}^0V + \int_{{}^0S_f} f_i^{\mathrm{S}}\frac{\partial u_i^{\mathrm{S}}}{\partial z_m}\,\mathrm{d}^0S \tag{38}$$

where z_m is the mth design variable. From Eq. (38), it is pretty straight-forward to think of calculating the mean compliance sensitivity by direct computation of the derivatives of the displacement field with respect to design variables, however, this direct method is not efficient. In our problem it is more economic to use the adjoint method to calculate the derivatives. In order to use the adjoint method, we construct a functional W^* as

$$\begin{aligned} W^* = W &+ \int_{{}^0V} S_{ij}^{\mathrm{a}}\left[\epsilon_{ij} - \frac{1}{2}\left(\frac{\partial u_i}{\partial^0 x_j} + \frac{\partial u_j}{\partial^0 x_i} + \frac{\partial u_k}{\partial^0 x_i}\frac{\partial u_k}{\partial^0 x_j}\right)\right]\mathrm{d}^0V \\ &+ \int_{{}^0V} \epsilon_{ij}^{\mathrm{a}}(S_{ij} - C_{ijkl}\epsilon_{kl})\,\mathrm{d}^0V + \int_{{}^0V} f_i^{\mathrm{B}}u_i^{\mathrm{a}}\,\mathrm{d}^0V \\ &+ \int_{{}^0S_f} f_i^{\mathrm{S}}u_i^{\mathrm{S,a}}\,\mathrm{d}^0S - \frac{1}{2}\int_{{}^0V} S_{ij}\left(\frac{\partial u_i^{\mathrm{a}}}{\partial^0 x_j} + \frac{\partial u_j^{\mathrm{a}}}{\partial^0 x_i}\right. \\ &\left. + \frac{\partial u_k^{\mathrm{a}}}{\partial^0 x_i}\frac{\partial u_k}{\partial^0 x_j} + \frac{\partial u_k}{\partial^0 x_i}\frac{\partial u_k^{\mathrm{a}}}{\partial^0 x_j}\right)\mathrm{d}^0V \end{aligned} \tag{39}$$

where S_{ij}^{a}, $\epsilon_{ij}^{\mathrm{a}}$ and u_i^{a} are parameters to be determined. Observe that Eq. (39) has terms corresponding to the strain–displacement relation of Eq. (2), the constitutive relation of Eq. (3) and the equilibrium Eq. (1) with the virtual displacement δu_i replaced by u_i^{a}, it is easy to prove that $W^* = W$. By taking the derivative of both sides of Eq. (39) and making use of Eq. (38), we have

$$\begin{aligned} \frac{\mathrm{d}W}{\mathrm{d}z_m} = &\int_{{}^0V}\frac{\partial S_{ij}}{\partial z_m}\left[\epsilon_{ij}^{\mathrm{a}} - \frac{1}{2}\left(\frac{\partial u_i^{\mathrm{a}}}{\partial^0 x_j} + \frac{\partial u_j^{\mathrm{a}}}{\partial^0 x_i} + \frac{\partial u_k^{\mathrm{a}}}{\partial^0 x_i}\frac{\partial u_k}{\partial^0 x_j}\right.\right. \\ &\left.\left. + \frac{\partial u_k}{\partial^0 x_i}\frac{\partial u_k^{\mathrm{a}}}{\partial^0 x_j}\right)\right]\mathrm{d}^0V + \int_{{}^0V}\frac{\partial \epsilon_{ij}}{\partial z_m}(S_{ij}^{\mathrm{a}} - C_{ijkl}\epsilon_{kl}^{\mathrm{a}})\,\mathrm{d}^0V \\ &+ \int_{{}^0V} f_i^{\mathrm{B}}\frac{\partial u_i}{\partial z_m}\,\mathrm{d}^0V + \int_{{}^0S_f} f_i^{\mathrm{S}}\frac{\partial u_i^{\mathrm{S}}}{\partial z_m}\,\mathrm{d}^0S \\ &- \frac{1}{2}\int_{{}^0V} S_{ij}^{\mathrm{a}}\left[\frac{\partial}{\partial^0 x_j}\left(\frac{\partial u_i}{\partial z_m}\right) + \frac{\partial}{\partial^0 x_i}\left(\frac{\partial u_j}{\partial z_m}\right)\right. \\ &\left. + \frac{\partial}{\partial^0 x_i}\left(\frac{\partial u_k}{\partial z_m}\right)\frac{\partial u_k}{\partial^0 x_j} + \frac{\partial u_k}{\partial^0 x_i}\frac{\partial}{\partial^0 x_j}\left(\frac{\partial u_k}{\partial z_m}\right)\right]\mathrm{d}^0V - \frac{1}{2} \\ &\times\int_{{}^0V} S_{ij}\left[\frac{\partial u_k^{\mathrm{a}}}{\partial^0 x_i}\frac{\partial}{\partial^0 x_j}\left(\frac{\partial u_k}{\partial z_m}\right) + \frac{\partial}{\partial^0 x_i}\left(\frac{\partial u_k}{\partial z_m}\right)\frac{\partial u_k^{\mathrm{a}}}{\partial^0 x_j}\right]\mathrm{d}^0V \\ &- \int_{{}^0V}\frac{\partial C_{ijkl}}{\partial z_m}\epsilon_{ij}^{\mathrm{a}}\epsilon_{kl}\,\mathrm{d}^0V \end{aligned} \tag{40}$$

We can get rid of the terms involving $\partial S_{ij}/\partial z_m$, $\partial \epsilon_{ij}/\partial z_m$ and $\partial u_i/\partial z_m$ by requiring S_{ij}^{a}, $\epsilon_{ij}^{\mathrm{a}}$ and u_i^{a} satisfy the following adjoint system

$$\epsilon_{ij}^{\mathrm{a}} = \frac{1}{2}\left(\frac{\partial u_i^{\mathrm{a}}}{\partial^0 x_j} + \frac{\partial u_j^{\mathrm{a}}}{\partial^0 x_i} + \frac{\partial u_k^{\mathrm{a}}}{\partial^0 x_i}\frac{\partial u_k}{\partial^0 x_j} + \frac{\partial u_k}{\partial^0 x_i}\frac{\partial u_k^{\mathrm{a}}}{\partial^0 x_j}\right) \tag{41}$$

$$S_{ij}^{a} = C_{ijkl}\epsilon_{kl}^{a} \tag{42}$$

$$\int_{{}_0V} S_{ij}^{a}\delta\epsilon_{ij}\,\mathrm{d}^0V + \frac{1}{2}\int_{{}_0V} S_{ij}\left(\frac{\partial u_k^{a}}{\partial^0 x_i}\frac{\partial\delta u_k}{\partial^0 x_j} + \frac{\partial\delta u_k}{\partial^0 x_i}\frac{\partial u_k^{a}}{\partial^0 x_j}\right)\mathrm{d}^0V = \int_{{}_0V} f_i^{B}\delta u_i\,\mathrm{d}^0V + \int_{{}_0S_f} f_i^{S}\delta u_i^{S}\,\mathrm{d}^0S \tag{43}$$

The terms involving $\partial u_i/\partial z_m$ was actually eliminated by setting $\delta u_i = \partial u_i/\partial z_m$ in Eq. (43). As a result, Eq. (40) becomes

$$\frac{\mathrm{d}W}{\mathrm{d}z_m} = -\int_{{}_0V}\frac{\partial C_{ijkl}}{\partial z_m}\epsilon_{ij}^{a}\epsilon_{kl}\,\mathrm{d}^0V \tag{44}$$

The above derivative calculations can be further simplified by employing the relation in Eq. (37), consider

$$C_{ijkl} = \frac{f'(z_m)}{f(z_m)}C_{ijkl} \tag{45}$$

and notice $S_{ij} = C_{ijkl}\epsilon_{kl}$, we have

$$\frac{\mathrm{d}W}{\mathrm{d}z_m} = -\frac{f'(z_m)}{f(z_m)}\int_{{}_0V} S_{ij}\epsilon_{ij}^{a}\,\mathrm{d}^0V \tag{46}$$

If we choose $\delta u_i = u_i^{a}$ in Eq. (1) and utilize the relation in Eq. (41), we obtain

$$\frac{\mathrm{d}W}{\mathrm{d}z_m} = -\frac{f'(z_m)}{f(z_m)}\left(\int_{{}_0V} f_i^{B}u_i^{a}\,\mathrm{d}^0V + \int_{{}_0S_f} f_i^{S}u_i^{S,a}\,\mathrm{d}^0S\right) \tag{47}$$

Eq. (47) is the basic expression for calculating the mean compliance sensitivity of geometrically nonlinear structures. The only unknown u_i^{a} represents the displacement field of the adjoint structure governed by Eq. (43). If we compare Eq. (43) with the linearized incremental equation of Eq. (11), we find that the adjoint structure is actually the tangent structure corresponding to the final deformed structure configuration, and the load applied upon the tangent structure is the same one acted on the physical structure. Since we already constructed the tangential stiffness matrix in the analysis part, it can be directly used to solve u_i^{a}. In the finite element formulation, Eq. (47) becomes

$$\frac{\mathrm{d}W}{\mathrm{d}z_m} = -\frac{f'(z_m)}{f(z_m)}\boldsymbol{R}^{T}\boldsymbol{u}^{a} \tag{48}$$

where $\boldsymbol{R}$ represents the applied nodal forces, $\boldsymbol{u}^{a}$ is the nodal displacement vector of the adjoint structure, which is calculated by the following linear equations

$$\boldsymbol{K}_{T}\boldsymbol{u}^{a} = \boldsymbol{R} \tag{49}$$

where $\boldsymbol{K}_{T}$ is the tangential stiffness matrix at the final structure configuration.

After the design sensitivity information for the objective function and constraints are calculated, the GCA method introduced by Chickermane and Gea [8] is used to formulate an approximated optimization problem and it is then solved iteratively using mathematical programming until the optimized layout is generated.

4. Numerical examples

4.1. Example 1

The first example considers the stiffness optimization design of a slender plate under a concentrated loading as shown in Fig. 1(a). The plate is fixed at central points of both sides and has length 0.8 m, width 0.2 m and

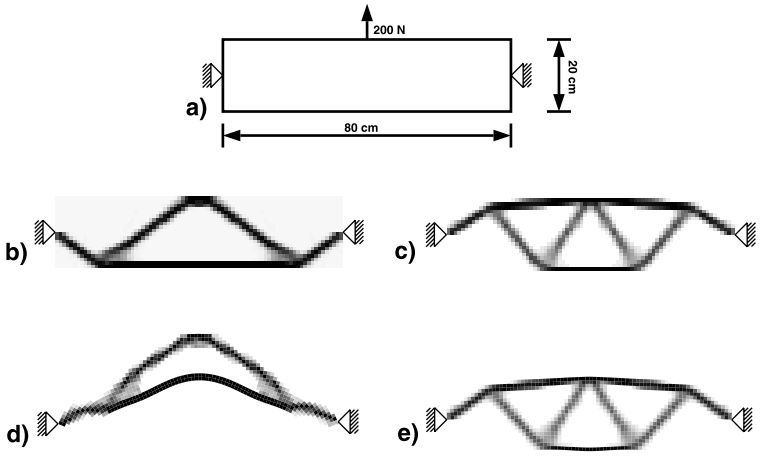

Fig. 1. Stiffness optimization of example 1. (a) Design domain and boundary conditions, (b) optimal topology obtained using linear finite element analysis, (c) optimal topology resulting from geometrically nonlinear finite element analysis, (d) deformation of topology b using geometrically nonlinear finite element analysis and (e) deformation of topology c using geometrically nonlinear finite element analysis.

thickness 0.1 cm, the force is applied upward at the top edge with the magnitude of 200 N. It is assumed that the available material can only cover 20% volume of the design domain, and the material has Young's Modulus 1 GPa and Poisson's ratio 0.3. Linear finite element analysis-based topology optimization was first carried out to find the linear design and the result is illustrated in Fig. 1(b). The nonlinear design obtained from the proposed method using the geometrically nonlinear finite element analysis is shown in Fig. 1(c) and exhibits significant difference from the linear one. In order to sort out which design is better, the structural deformations of both layouts are calculated using the nonlinear finite element analysis, and as a result, Fig. 1(d) shows the deformation of the linear design, and Fig. 1(e) shows the deformation of the nonlinear design. It can be seen that the linear design experiences large deformation under the applied force, whereas the nonlinear design has only very slight displacement variation implying a much stiffer design. Compared with 3.1399×10^3 N m mean compliance of the linear design, the mean compliance of the nonlinear design drops nearly seven times to 4.2192×10^2 N m. It goes without saying that the geometrically nonlinear finite element analysis is necessary to find the optimal design of the large displacement structure.

4.2. Example 2

In the second example, we consider the design problem sketched in Fig. 2(a). The plate is clamped on both sides, and three concentrated forces are acted upward on its bottom edge with the value of 15, 30 and 15 N respectively. The dimension of the plate is defined as 80 cm × 20 cm × 0.1 cm. Suppose only 20% of design domain volume material is available for constructing the final structure and the material has Young's Modulus of 100 MPa, Poisson's ratio of 0.3. The design topology using the linear analysis is shown in Fig. 2(b) and the design from the nonlinear analysis is given in Fig. 2(c). Once again, these two designs exhibit disparities to a great extent. Fig. 2(d) and (e) shows the deformations of the linear and nonlinear designs under the applied forces, and the corresponding mean compliances are 7.4323×10^2 and 1.1950×10^2 N m respectively. Obviously, the nonlinear design is much stiffer and produces a true optimal design for this specific large displacement problem, on the contrary, the linear design fails to find the optimal one but generates a fake optimal design which may not survive the originally set design constraints.

4.3. Example 3

In the third example, the same design problem as in the second example is considered except that we changed the magnitudes and directions of the applied forces. The forces are now acted downward and their magnitudes have been changed proportionally to 200, 400 and 200 N respectively, the design problem is sketched in Fig. 3(a). Fig. 3(b) and (c) shows the design layouts from the linear analysis and the nonlinear analysis. If we compare the linear design with the one of Fig. 2(b) in the second example, we find the two designs are exactly the same, however the nonlinear design is totally different from its counterpart in the second example. This observation

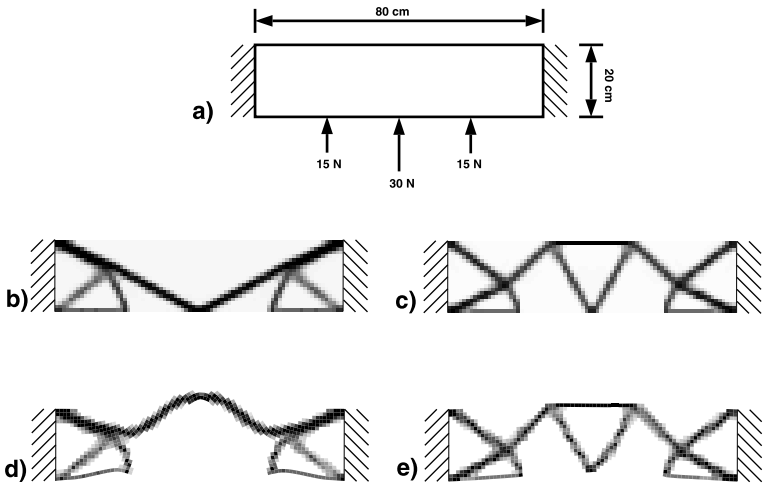

Fig. 2. Stiffness optimization of example 2. (a) Design domain and boundary conditions, (b) optimal topology obtained using linear finite element analysis, (c) optimal topology resulting from geometrically nonlinear finite element analysis, (d) deformation of topology b using geometrically nonlinear finite element analysis and (e) deformation of topology c using geometrically nonlinear finite element analysis.

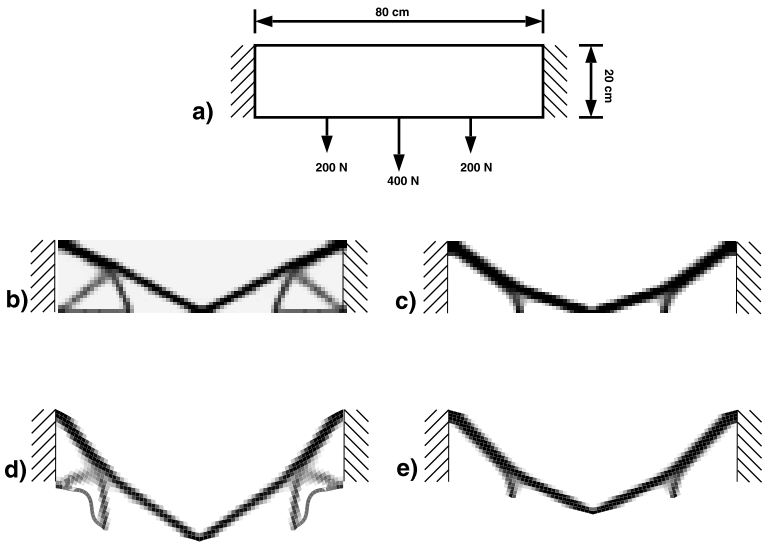

Fig. 3. Stiffness optimization of example 3. (a) Design domain and boundary conditions, (b) optimal topology obtained using linear finite element analysis, (c) optimal topology resulting from geometrically nonlinear finite element analysis, (d) deformation of topology b using geometrically nonlinear finite element analysis and (e) deformation of topology c using geometrically nonlinear finite element analysis.

reveals a significant difference between the linear analysis and the nonlinear analysis: for the linear analysis, the displacement is a linear function of the applied load, since the loads between the two examples are proportional, the two resulting displacement fields are proportional too, which means the layout opted for one case must be opted for the other; in the nonlinear analysis, however, the displacement is a nonlinear function of the applied load, there are no similarities between individual displacement fields even though their loads are proportional, which unarguably leads to irrelevant designs. The deformations of the linear and nonlinear designs are shown in Fig. 3(d) and (e) with the mean compliance of 9.8050×10^3 and 5.0461×10^3 N m, respectively. It's obvious that the nonlinear design is much stiffer than the linear one, showing that for large displacement problems, the geometrically nonlinear finite element analysis is indispensable for the structural optimization.

5. Conclusion

In this paper, the stiffness optimization problem of geometrically nonlinear structures is studied. The mean compliance of the structure is chosen as the objective function and its sensitivities are derived using the adjoint method. From the derivations, the relations between the mean compliance, the strain energy and the complementary strain energy are discussed. The optimal problem is formulated using a microstructure-based design domain method and is solved iteratively by a sequential convex approximation method. Numerical results demonstrate that for structures involving large displacement or large rotation, the geometrically nonlinear finite element analysis must be incorporated into the structural optimization process, the regular linear finite element analysis may result in phony optimal designs and therefore must be proceeded with caution.

References

[1] Ananthasuresh GK, Kota S. The role of compliance in the design of MEMS. Proceedings of the 1996 ASME Design Engineering Technical Conferences, 96-DETC/MECH-1309.
[2] Bathe KJ. Finite element procedures. Englewood Cliffs, NJ: Prentice-Hall; 1996.
[3] Bendsøe MP, Kikuchi N. Generating optimal topologies in structural design using a homogenization method. Computer Meth Appl Mech Eng 1998;71:197–224.
[4] Bendsøe MP. Optimal shape design as a material distribution problem. Struct Optimization 1989;1:193–202.
[5] Bendsøe MP. Optimization of structural topology, shape, and material. Berlin: Springer; 1995.
[6] Bruns TE, Tortorelli DA. Topology optimization of geometrically nonlinear structures and compliant mechanisms. Short Paper Proceedings of 3rd World Congress of Structural and Multidisciplinary Optimization. 1999;1:1–3.
[7] Buhl T, Pedersen CBW, Sigmund O. Designing geometrically non-linear structures using topology optimization. Short Paper Proceedings of 3rd World Congress of Structural and Multidisciplinary Optimization. 1999;1:7–9.

[8] Chickermane H, Gea HC. A new local function approximation method for structural optimization problems. Int J Numeric Meth Eng 1996;39:829–46.
[9] Diaz AR, Kikuchi N. Solutions to shape and topology eigenvalue optimization problems using a homogenization method. Int J Numeric Meth Eng 1992;35:1487–502.
[10] Eshelby J. The determination of the elastic field of an ellipsoidal inclusion and related problems. Proceedings of the Royal Society, 1957;A241:379–96.
[11] Gea HC. Topology optimization: A new micro-structure based design domain method. Comput Struct 1996;61:781–8.
[12] Gea HC, Luo JH. Automated optimal stiffener pattern design. Mech Struct Mach 1999;27:275–92.
[13] Luo JH, Gea HC. Modal sensitivity analysis of coupled acoustic-structural systems. J Vibr Acoust 1997;119:545–50.
[14] Luo JH, Gea HC. Optimal bead orientation of 3D shell/plate structures. Finite Elements Anal Design 1998;31:55–71.
[15] Luo JH, Gea HC. A systematic topology optimization approach for optimal stiffener design. Struct Optimization 1998;16:280–8.
[16] Ma ZD, Kikuchi N, Hagiwara I. Structural topology and shape optimization for a frequency response problem. Comput Mech 1993;13:157–74.
[17] Mori T, Tanaka K. Average stress in matrix and average elastic energy of materials with midfitting inclusions. ACTA Metallurg 1973;21:571–4.
[18] Neves MM, Rodrigues HC, Guedes JM. Generalized topology design of structures with a buckling load criterion. Struct Optimization 1995;10:71–8.
[19] Rozvany GIN, Zhou M. Application of the COC method in layout optimization. In: Eschenauer H, Matteck C, Olhoff N, editors. Proceedings of International Conference of Engineering Optimization in Design Processes, 1990. p. 59–70.
[20] Seyranian AP, Lund E, Olhoff N. Multiple eigenvalues in structural optimization problems. Struct Optimization 1994;8:207–27.
[21] Sigmund O. On the design of compliant mechanisms using topology optimization. Mech Struct Machines 1997;25:495–526.
[22] Suzuki K, Kikuchi N. A homogenization method for shape and topology optimization. Computer Meth Appl Mech Eng 1991;93:291–318.
[23] Weng GJ. Some elastic properties of reinforced solids, with special reference to isotropic ones containing isotropic inclusions. Int J Eng Sci 1984;22:845–56.
[24] Yang RJ, Chen CJ, Lee CH. Bead pattern optimization. Struct Optimization 1996;12:217–21.